Optical nonlinearities and carrier transport in GaAs:EL2 at high excitation levels

Kestutis Jarašiunas, Philippe Delaye, Gérald Roosen

▶ **To cite this version:**

Kestutis Jarašiunas, Philippe Delaye, Gérald Roosen. Optical nonlinearities and carrier transport in GaAs:EL2 at high excitation levels. physica status solidi (b), 1993, 175, pp.445-457. 10.1002/pssb.2221750216 . hal-00686028

HAL Id: hal-00686028

https://hal-iogs.archives-ouvertes.fr/hal-00686028

Submitted on 6 Apr 2012

HAL is a multi-disciplinary open access archive for the deposit and dissemination of scientific research documents, whether they are published or not. The documents may come from teaching and research institutions in France or abroad, or from public or private research centers.

L'archive ouverte pluridisciplinaire **HAL**, est destinée au dépôt et à la diffusion de documents scientifiques de niveau recherche, publiés ou non, émanant des établissements d'enseignement et de recherche français ou étrangers, des laboratoires publics ou privés.

OPTICAL NONLINEARITIES AND CARRIER TRANSPORT IN GaAs:EL2 AT HIGH EXCITATION LEVELS

Kestutis Jarasiunas[*] *, Philippe Delaye and Gérald Roosen*

Institut d'Optique Théorique et Appliquée,
Unité de Recherche Associée 14 au Centre National de la Recherche Scientifique
Centre Scientifique d'Orsay, B.P. 147, 91403 ORSAY Cedex, France

Subject Classification : 72.20, 72.40, 77.50, 78.20, S.7.1

Abstract. Laser induced picosecond transient gratings are used to study carrier transport via free carrier and photorefractive nonlinearities in semi-insulating undoped GaAs bulk crystals. Carrier lifetime (τ_R=1.5 ns), hole and ambipolar mobilities (μ_h=410 $cm^2V^{-1}s^{-1}$, μ_a=760 cm^2 $V^{-1}s^{-1}$) are measured directly and electron mobility equal to 5200 cm^2 $V^{-1}s^{-1}$ is calculated. The optical properties of highly excited GaAs reveal deep donor EL2 transformation and intracenter absorption under picosecond excitation. Rotation of diffracted beam polarization is observed for the first time in orientation of grating vector along crystallographic axis (001) and attributed to a strain field at dislocations in LEC-grown GaAs wafers.

Résumé. La diffraction de la lumière sur les réseaux de porteurs libres et photoréfractif engendrés par des impulsions picoseconde permet d'étudier les non-linéarités optiques ainsi que le transport des porteurs libres dans le GaAs semi-isolant. Le temps de vie (τ_R=1.5 ns), la mobilité des trous et la mobilité ambipolaire (μ_h=410 $cm^2V^{-1}s^{-1}$, μ_a=760 cm^2 $V^{-1}s^{-1}$)) sont mesurés directement ; la valeur de la mobilité des électrons en est déduite (μ_n=5200 cm^2 $V^{-1}s^{-1}$). Les propriétés optiques du GaAs sans fortes excitations révèlent les transformations du niveau profond EL2 et l'absorption intracentre sans excitation picoseconde. Une rotation de la polarisation du faisceau diffracté est observée pour la première fois avec un vecteur réseau orienté suivant l'axe cristallographique (001). Ce signal est attribué à un champ de contrainte à longue distance autour des dislocations dans le GaAs fabriqué par la technique LEC.

---

[*] On leave from Material Research Laboratory "INTEST", Semiconductor Physics Department, Vilnius University, Sauletekio all. 9, Bld. 3, 2054 Vilnius Lithuania

1. Introduction.

Numerous experiments on nonlinear optical phenomena in semi-conductors have been performed using transient grating techniques /1-3/. Most of previous studies used band-to-band bipolar carrier plasma generation to create free carrier in Si, Ge, A_2B_6, A_3B_5 compounds by one or two-photon absorption of light. Time resolved grating decay measurements of self-diffracted beam intensity characteristics revealed carrier diffusion and recombination processes in pure crystals, carrier generation and transport peculiarities due to doping by shallow impurities, ion irradiation, external electric fields /4/. Possible applications of this technique in the fields of material research have been shown /5/.

In recent years, studies of optical nonlinearities in photorefractive crystals have been carried out in picosecond time scale /6-12/. In this kind of crystals photorefractive and non-photorefractive nonlinearities may take place simultaneously. Here a large variety of carrier generation mechanisms exists (absorption from deep levels, both single two-step processes from deep levels and two photon absorption) which finally will determine the magnitude and dynamics of these nonlinearities. Experiments in undoped CdTe crystals have revealed the role of Dember field in the enhancement of the photorefractive effect /8,9/ and the contribution of this nonlinearity to thin grating decay kinetics /10/. In vanadium-doped CdTe the separation of free carrier (FC) and photorefractive (PR) contributions allowed to measure monopolar and bipolar carrier mobilities and to observe a space-charge field feed-back effect on carrier transport /11,12/.

In order to explain peculiarities of optical nonlinearities described in these works, further theoretical and experimental investigations of carrier transport and of space-charge field dynamics in photorefractive semiconductors are necessary. We thus continue this kind of experimental studies on picosecond time scale in highly excited GaAs crystals.

The sample used was a nominally undoped semi-insulating GaAs crystal, grown by the liquid encapsulated Czochralski (LEC) technique /13/. The crystal was cut with the faces along the crystallographic directions (110), (-110), and (001). The absorption coefficient of 1.5 mm thick sample was found equal to 1 cm^{-1} at 1.06 μm. It is well known that the dominant defect in undoped material is an intrinsic deep donor level EL2 and it solely determines the absorption at 1.06 μm /14, 15/. In this way we estimated deep donor concentration in our sample as $NEL2=1.5\ 10^{16}\ cm^{-3}$, being a typical value for LEC-grown GaAs crystals /16/.

The configuration of the experimental set-up was a degenerate four-wave mixing scheme (figure 1). Using the Yag-laser with pulse duration τ_L=28 ps FWHM and output energy up to 10 mJ.cm^{-2}, gratings with period Λ=1.8 μm were recorded by two s-polarized beams. The polarization states of transmitted probe beam and of diffracted one were monitored at different orientations of grating vector K_g with respect to sample crystallographic axis. In this way a contribution of a PR nonlinearity was separated from a coexisting and much stronger FC non linearity /8,17/. The cases when pure PR grating (i.e. p-diffracted component of s-polarized probe beam for K_g //(110)) or pure FC grating (i.e. p-diffracted component of p-polarized probe beam at K_g //(110)) were analyzed experimentally. A $\lambda/2$ plate was used for selecting the probe beam polarization (p or s) (figure 1). A Glan polarizer oriented to reflect p-polarization was used for separation of Bragg-diffracted beam counterpropagating to one of recording s-polarized beams. Then the diffracted beam was directed to a fast silicon photodiode through the next p-transmitting polarizer. Such a set-up allowed us to realize a noise-free interferometer able to detect diffracted signals as low as 10^{-6} - 10^{-7}. Diffracted beam intensity I_1 or grating efficiency $\eta = <I_1> / <I_T>$ (here $<I_1>$ and $<I_T>$ are time-integrated values of diffracted and transmitted probe beams) as a function of excitation level I and of probe beam delay time Δt were studied. Sample transmittivity kinetics $<I_T> = f(\Delta t)$ were also measured at different excitation levels or probe beam polarizations in order to analyze light absorption mechanisms and their peculiarities.

2. Exposure characteristics.

The exposure characteristics (EC) of a semiconductor (i.e. dependence of the diffracted beam intensity $<I_1>$ versus excitation energy I) contains the main information about carrier generation processes. If light induced changes of optical properties are small enough (diffraction efficiency $\eta < 0.01$), EC follows a power law dependence, $<I_1> = I^{\gamma}$/18/. Assuming that carrier concentration increases with excitation as $N = I^{\beta}$, the following relationship between slopes γ and β in log-log scale results /18,19/.

$$<I_1> = <I_T> \left(\pi \Delta n d / \lambda\right)^2 = I_p T \left(\pi n_{eh} \Delta N d / \lambda\right)^2 = A\ I^{2\beta+1} = A I^{\gamma} \qquad (1)$$

here ΔN is the modulated FC concentration, n_{eh} is the refractive index change due to one electron-hole pair according to Drude model /1/, d is the thickness of the sample, and I_p is the probe beam intensity. In this way the carrier generation rate parameter β can be easily obtained /18, 19/.

In a general case, a linear carrier generation with β= 1 will lead to γ = 3 and, correspondingly, two-step and two-photon light absorption (β=2) will increase the slope of EC

to γ=5. In our semi-insulating undoped sample we observed increase of EC slope with value γ_1=3.9 at excitation levels below 4 mJ.cm^{-2} both for FC and PR gratings (Fig. 2, 3). From the experimental value of γ_1 we estimated parameter of carrier generation rate β_1~1.5 according to relationship given by equ. (1). This value of β_1 is determined by linear electron generation from deep EL2 traps which is altered due to nonlinear mechanisms of bipolar carrier plasma creation (i.e. by two-step transitions via ionized EL2 traps and by two-photon absorption). Diffraction efficiencies $\eta = I_1/I_T = 4.10^{-3}$ and 4.10^{-5} and for FC and PR gratings respectively were reached at excitation level 4 mJ.cm^{-2}, and the following values of light induced refractive index modulation were thus estimated : $\Delta n^{FC}=2.10^{-5}$ and $\Delta n^{PR}=2.10^{-6}$ (at the end of excitation pulse, when $\Delta t = \tau_L$). Assuming that the refractive index changes are due to FC concentration ΔN and space charge field E_{sc}, the following absolute values of $\Delta N = 6.10^{15}$ cm^{-3} and E_{sc}=2000 V.cm^{-1} were calculated and used in the further analysis of results.

At excitation levels above 4 mJ.cm^{-2} a strong decrease of EC slope was observed (Fig. 2, $\gamma_2 = 1.7$ for FC grating), and corresponding value of sublinear carrier generation rate β_2=0.5 was estimated. At these excitation levels PR grating also exhibits a slowering in space charge field creation with excitation (Fig. 3). In addition, exposure characteristics of sample transmittivity (Fig. 2, 3) revealed an increasing light induced absorption with excitation. These features alltogether point out that a new mechanism of light absorption at 1.06 μm in picosecond time scale dominates what leads to quenching of FC and PR gratings diffraction efficiency /20/.

Time resolved measurements of induced absorption have been carried out to investigate its origin. We observed time-resolved structure of sample transmittivity : a bleaching on the front edge of pulse and a subsequent darkening with at least two components of the latter process (Fig. 4). The first component of darkening evolves as an integral of excitation pulse, reaches the value $\Delta\alpha$=3-4 cm^{-2} and relaxes in 100 ps. Then the next competing component is arising, which reaches $\Delta\alpha$=1-1.5 cm^{-1} and relaxes with time constant of 5-10 ns. This behaviour of transmitted beams was observed both for p- and s-polarized probe beams but the time-resolved structure was more evident in the latter case.

The origin of small bleaching at low excitation is due to partial deep level depletion what has been observed in previous works /6, 21, 22/. But the peak of induced absorption can not be explained neither by free carrier intraband absorption /23, 24/ nor by transitions between intervalence bands /25/. Peculiarities of two-photon absorption in transient energy transfer and in transmittivity were carefully examined /6/ but this mechanism is not able to explain the features of our experiment : delayed position of transmittivity maximum, its fine structure, and long tail of relaxation.

We ascribe this complicated dynamics of transmittivity and of diffraction quenching to deep EL2 trap related transitions under powerful picosecond excitation. Two kind of processes must be considered at excitation wavelength of 1.06 μm : (i) intracenter absorption in deep EL2 traps which does not affect the concentration of free electrons /26, 27/ and/or (ii) transformation of EL2+ to doubly ionized state EL2++ /28,29/. Our experiments provide some arguments that both processes may take place. First, the energy range for intracenter transition with its maxima at 1.18 eV /26/ corresponds to the laser wavelength used in our experiment ; next, this process is supposed to be non-photoactive /27/ what is identified from the quenching of diffraction efficiency. Moreover, photon capture cross section for this transition is quite large /26/ (about 10^{16} cm^2). This transition to a non-photoactive state without charge generation is assumed to be the first step in a chain of processes leading to metastable state creation /30/. From ref. 24, the rate of desexcitation of this transient non-photoactive state is supposed to be very fast at room temperature /24/ and is followed by hole generation. Thus the mechanism of intracenter transitions might explain diffraction quenching and a fast relaxation of induced absorption but not the full value of it.

For the second process (ii), transformation of EL2+ to EL2++ states may be assumed as a new channel of light absorption which lowers the part of fluence used for efficient electron generation from neutral donor states. Again, if transformation to EL2++ and its recovery to EL2+ take place during the action of the laser pulse, this will result in more efficient generation of holes because the optical cross section for transfer from EL2++ to EL2+ ($\sigma_{p2} \sim 6.10^{-17} cm^2$ /28-29/) is larger than one from EL2+ to ground state ($\sigma_{p1} \sim 2.10^{-17} cm^2$ /21/). As a result, one would also observe an increasing absorption and decreasing diffraction efficiency.

The observed processes of induced absorption due to intracenter transitions and EL2 transformation under picosecond excitation also might explain the variation in measured ratio of the hole cross section to electron cross section for the EL2 defect in undoped semi-insulating GaAs /24/. At low excitation levels this ratio was found varying from 0.1 to 0.25 (see /24/ and Ref. therein), but at picosecond excitations it increased to 0.8-1 /24/. The latter increase may result from activation of more efficient channels of hole generation via highly excited EL2 system.

In summary, we conclude that the simultaneous studies of light diffraction on FC and PR gratings as well as of dynamics of transmittivity have revealed different light absorption mechanisms, and, thus, may serve as a tool for further investigation of EL2 defect transformation features with excitation. The appearence of new states will cause modification of carrier generation rates, and of the built-in electric field ; in this way, creation and dynamics of PR and FC gratings will be affected. These features will be analyzed below from the transient grating decay measurements at different excitation levels.

3. Time-resolved grating decay.

3.1. Free carrier gratings (Kg//(110))

At low excitation levels, when $0.8 < I < 2.5$ mJ.cm^{-2}, we observed two components in grating decay, τ_{e1} and τ_{e2}, both varying with the excitation in the intervals 80 ps $< \tau_{e1} <$ 160 ps and 30 ps $< \tau_{e2} <$ 60 ps (grating decay time corresponds to time interval $\Delta t = \tau_e$ when diffracted signal decreases to level e^{-2}). Decay times slower with excitation, and the first component shows tendency to saturation (fig. 5). At fluences $I > 3$ mJ/cm^2 grating decay starts with the time constant τ_{e2}=50-60 ps, which with the further increase of excitation approaches its shortest value observed in our experiments, namely, 42-43 ps (Fig. 6a). Moreover, this decay is followed by a slower part with a new time constant τ_{e3}=110-120 ps, and finally long lasting component of grating decay with τ_{e4}=1.5 ns appears (Fig. 6b).

The carrier dynamics must be analyzed taking into account light created space charge (SC) field and its feed-back effect to carrier transport /12/. At low excitations, electron diffusion will decrease the grating modulation depth with time constant of 6 ps, in this way creating SC field. The latter will slower or even stop carrier diffusion in this way preventing grating from its total decay /11/. The diffusion of holes during the action of laser pulse can be neglected due to their low mobility. After the pulse is over and electron grating has been partly erased, hole diffusion and drift become the dominant processes of grating decay. The diffusion will follow carrier bipolar mobility according to the well known relation :

$$\mu_a = (N + P) / \left(P / \mu_e + N / \mu_p\right) \tag{2}$$

which in our conditions (N >> P, thus excess holes diffuse in a n-type crystal) leads to $\mu_a=\mu_p$. The carrier will drift with an effective mobility μ^* :

$$\mu^* = (N - P) / \left(P / \mu_e + N / \mu_p\right) \tag{3}$$

which also has a limit value $\mu^*=\mu_p$ under above conditions (N >> P at low excitation). The dependences of diffusion and drift related grating decay times (with Λ = 1.8 μm) calculated according to eq. 2 and eq. 3 are shown in Fig. 7. Thus, the first component of FC grating decay observed at the lowest excitations, τ_{1e}=80 ps, corresponds to hole drift in SC field and gives the value μ^*=410 cm^2.V^{-1}.s^{-1} from the expression of grating decay time due to drift : $\tau_{DRIFT}=1/K_g E_{sc}\mu^*=\tau_{1e}$. At higher excitations, holes are generated more efficiently, and hole drift slowers : the observed $\tau_{1e} \approx$ 100–160 ps corresponds to an N/P ratio varying from 6 to 2 with excitation (see eq. 3). Finally the drift component is saturated when N = P.

Hole drift with respect to the ionic grating will cause a decrease of SC field, and the diffusive current increases. Thus the second component of FC grating decay is a diffusion of a remaining electron grating (at low excitations) or bipolar electron-hole plasma diffusion (at high excitations) ; for the latter case, when N=P, we derive μ_a = 760 $cm^2\ V^{-1}s^{-1}$ and correspondingly $\tau_{e2} = 43$ ps. This qualitative model explains quite well the observed averaged time constants of grating decay, wich depend on the N/P ratio at a given excitation. In fact, the processes of diffusion and drift do not equilibrate independently, and the dynamics of grating modulation due to SC field feed-back effect is more complicated (especially at lower fluences, when electron-like grating is created).

The time required for holes to drift a distance $x = \Lambda/2$ is estimated as 250 ps. In this way a π-shifted from the former position hole grating will be created /21/ and its relaxation may be observed. Experimentally we indeed found the appearance of a new grating decay component τ_{e3}. Grating decay in this time domain is nonmonotonous and modulated by a faster one : possibly, there is a competition of a simultaneously existing π-shifted hole grating and an electron grating reconstructed by the SC field. Even at a small modulation depth of the latter grating, its influence may be significant due to a much more efficient refractive index modulation by the electron concentration than by the hole one (the refractive index modulation coefficient by electrons is much larger than by holes : according to Drude model, this ratio is proportionnal to the inverse ratio of carrier effective masses, i.e. approximately to 10).

We attribute the last component of the grating decay with $\tau_{e4} \approx 1.5$ ns (Fig. 6) to the relaxation of an amplitude grating which is formed in EL2 traps due to their spatial photoionization. This trap modulation will be maintained until recombination of free carriers will reconstruct the initial neutral trap density. Thus, carrier lifetime is deduced directly from this relaxation, $\tau_R=\tau_{e4}$. In addition, we estimated the value of the absorption coefficient modulation from the amplitude of the grating efficiency $\eta = (\Delta\alpha d / 2\cos\theta)^2 \approx 2.10^{-5}$ at $\Delta t \approx 300ps$. This experimental value $\Delta\alpha_{exp} \approx 0.09cm^{-1}$ is in good agreement with the calculated one $\Delta\alpha$=0.1 cm^{-1} deduced from the product of initial trap density N_{EL2} and their effective cross-section at high excitations $\left[\sigma_n\sigma_p / (\sigma_n + \sigma_p)\right]$ /17/. In this way the origin of amplitude modulation is confirmed.

The strong induced absorption observed in transmittivity should lead to creation of an amplitude grating with $\Delta\alpha d$ = 0.2 - 0.4 in time interval Δt = 100 - 300 ps. Experiments have not revealed such a grating neither with corresponding amplitude nor with relaxation time correlating with recovery of transmittivity. This behaviour may be explained only in one way : the darkening induced at grating maxima becomes rapidly homogeneous along the grating vector This is possible if this darkening is due to mobile species which distribute

homogeneously in some hundreds of picoseconds, and that these species are not creating significant refractive index modulation. Thus, generation of free holes might explain negligible influence of amplitude grating to diffraction efficiency. Computer simulation of processes involved in absorption of light and modulation of optical properties will give more detail insight into observed peculiarities.

3.2. Photorefractive gratings (K_g //(110)).

We observed two components of pure PR grating decay, varying with excitation in a similar way as we have found for FC gratings.

At low fluences, SC electric field between positive charge at grating maxima (ionized donors and holes) and negative charge in grating minima (electrons transfered there by diffusion from grating maxima) is established very fast. Hole drift in this SC field is expected to be the next step in charge and field dynamics. The estimated value of PR grating decay at N >> P, according to eq. 3 and fig. 7, equals to 80 ps. This value correlates well with the experimental one τ_{e1}=80ps, the first component of FC grating decay at the lowest excitations. There is clear tendency of a grating decay slowering with excitation, and the values of 120 ps < τ_{e1} < 240 ps have been measured (Fig. 8a). This is consistent with the decrease of drift mobility with increasing N/P ratio (eq. 3), and the corresponding ratio N/P varying from 3.5 to 1.5 was estimated from the measured decay times.

At delay times larger than 60 ps, the speed of decay increased and was below our temporal resolution, being limited by duration of the laser pulse, i.e. $\tau_{e2} < \tau_L$. This observation and the temporary oscillations of diffracted beam intensity at low excitations (Fig. 8a) point out that very fast processes are involved in SC field modulation. Similar perculiarities were found for picosecond PR gratings in CdTe and GaAs and attributed to carrier transport in nonhomogeneous electric fields or to hot carrier enhanced diffusion /9, 12/.

At higher excitation levels (I ~5 mJ.cm^{-1}) grating decay has a smoother profile : the time domain, where τ_{e1} dominates, is compressed, and decay starts with the second components τ_{e2}, reaching values of 44-48 ps (Fig. 8b). This time constant at given grating period corresponds to ambipolar diffusivity of carrier plasma with N/P ratio varying from 1 to 1.3. This time constant indicates that Dember field between mobile species dominates and governs grating decay. Again, when diffraction efficiency drops to level of 10^{-5}, the decay is faster and corresponds to the case $\tau_{e2}<\tau_L$.

Direct determination of monopolar mobilities is possible from the experimental data of PR and FC grating decay times measured at different fluences. First, hole diffusion coefficient

D_h=10.2 $cm^2.s^{-1}$ and mobility μ_h=400-410 $cm^2.V^{-1}.s^{-1}$ are derived from the measured decay time τ_{1e}^{FC}=80 ps at Λ=1.8 μm. Next, the shortest limit of ambipolar decay τ_{3e}^{PR}=43-44 ps leads to the values of ambipolar diffusion coefficient D_a=18.6 - 19 $cm^2.s^{-1}$ as well as of ambipolar mobility $\mu_a \approx 760$ $cm^2.V^{-1}.s^{-1}$. Thus, the electron mobility may be estimated from our measurements, and the value $\mu_e \approx 5200$ $cm^2.V^{-1}.s^{-1}$ was obtained.

3.3. Gratings at K_g//(001).

The photorefractive signal in the case K_g//(110) is usually separated from the nonphoto-refractive one by using the effect of polarization rotation of linearly polarized probe beam to the orthogonal one /12, 17, 31/. Another usual test procedure to confirm the photorefractive origin of the refractive index modulation is the crystal rotation by 90° (so that crystallographic (001) axis is parallel to the grating wave vector K_g) and subsequent measurement of p-polarized component of the diffracted beam using s-polarized probe beam. No signal is to be observed in the latter case, and this was reported in number of experiments on semi-insulating CdTe and GaAs samples /8, 9, 12/.

In contrary, to this expectation, we have here observed a strong p-polarized diffracted signal from a grating oriented with K_g//(001) and probed by a s-polarized beam. The diffracted signal reached values of η up to 10^{-4} at the end of the excitation pulse, being of the same intensity as for the studied above photorefractive geometry. To test leakage of separation-detection system, we inserted a p-Si sample (ρ ≈ 10 Ω cm) instead of the GaAs, and found no signal. Moreover, using the same set-up, no diffracted signal was observed in photorefractive CdTe:V sample (or η value was below 10^{-7} in the case K_g //(001)) while for photorefractive orientation K_g//(110), the value of $\eta_{PR} = 7.10^{-5}$ has been measured /12/.

The preliminary studies of the origin of the observed effect have been carried out. The measurements of the grating decay at different fluences has revealed three components : the first one, related to hole drift and its saturation with excitation, the second one, relaxing with the time of ambipolar diffusivity, and the last component of decay with $\tau_e \leq \tau_L$. These data indicate that the behaviour of the optical nonlinearity in K_g//(001) is similar to the one for a typical photorefractive case studied above (i.e. in orientation K_g//(110)) and, thus, give strong arguments towards the identification of a photorefractive origin of the grating in orientation K_g//(001).

One of possible mechanisms that leads to photorefractive modulation mechanism is bulk photovoltaic effect in media containing macroscopic inhomogeneities which act as local space charges /32/. Indeed, LEC-grown semi-insulating GaAs crystals exhibit specific macroscopic distribution of dislocations /13, 16/ which are able to getter intrinsic defects. The concentration

of midgap EL2 centers duplicates almost exactly the characteristic dislocation distribution pattern /5, 13/. The local region around dislocations (or order 30-50 μm) is perturbated : the inhomogeneous stress field and electric field accompany the dislocations /33/, which in semi-insulating GaAs are charged by electrons from EL2 centers /33, 34/. These fields may break the crystal symmetry, and non-zero components of the electrooptic tensor will appear. From the other hand, the existence of dislocation bands and bound states /33, 34/ may cause carrier confinement, anomalies in carrier transport, and new photovoltaic effects /32/. These proposed models will be worked out by further studies of optical and electrical activity of defects in LEC-grown GaAs crystals with different dislocation densities.

4. Conclusion.

We have demonstrated novel possibilities of dynamic grating techniques to study carrier transport peculiarities via free carrier and photorefractive nonlinearities. Carrier generation and transport have been found strongly dependent on excitation level, and grating decay measurements at different fluences allowed direct determination of monopolar and bipolar mobilities, lifetime. Strong induced absorption and its non-photoactive features have been found at high excitation levels and discussed in terms of EL2 level transformation in picosecond time domain. Light diffraction with photorefractive features has been found in orientation K_g//(001). This previously not observed phenomenon was attributed to long-range internal strain and electric fields at dislocations in LEC-grown bulk GaAs crystals.

Acknowledgments. Kestutis Jarasiunas thanks the Ministère de la Recherche (France) for his financial support and is very grateful to the Institut d'Optique where he spent his research stay.

REFERENCES

1. R.K.Jain and M.B.Klein, "Degenerate Four-Wave Mixing in Semiconductors" in: Optical Phase Conjugation . New York: Acad. Press, 1983, pp. 307-415.

2. A.Miller, D.A.B.Miller, and S.D.Smith, Adv. in Phys., vol. 30, pp.697-800, 1981.

3. H.J.Eichler, P.Gunter, and D.W.Pohl. Laser Induced Dynamic Gratings , Springer Ser. Opt. Sci. Vol 50, Berlin-Heidelberg, 1986.

4. J.Vaitkus, K.Jarasiunas, E.Gaubas, L.Jonikas, R.Pranaitis, and L.Subacius, IEEE J. Quantum Electron., **QE-22**, pp.1298-1305, 1986.

5. J.Vaitkus, E.Gaubas, K.Jarasiunas, and M.Petrauskas, Semicon. Sci. Technol., **7**, p. A131-A134, 1992.

6. A.E.Smirl, G.C.Valley, K.M.Bohnert, and T.F.Boggess, Jr., IEEE J. Quantum Electron., **QE-24**, p. 289 -303, 1988.

7. G.Pauliat and G.Roosen, J. Opt. Soc. Am. B, **7**, p.2259, 1990.

8. W.A.Schroeder, T.S.Stark, M.D.Dawson, T.F.Boggess, A.L.Smirl, and G.C.Valley, Opt.Lett., **16**, p.159-161, 1991.

9. W.A.Shroeder, T.S.Stark, and A.L.Smirl, Opt. Lett, **16**, p.989-991, 1991.

10. I.Ruckmann, J.Kornack, J.Kolenda, M.Petrauskas, Y.Ding, and B.Smandek, phys. stat. sol. (b), **170**, 353, 1992.

11. K.Jarasiunas, P.Delaye, J.C.Launay, and G.Roosen, Proceedings of Int. Conf. on Electron. Materials (ICEM-92), Strasbourg, 1992, paper F-VIII.3.

12. K.Jarasiunas, P.Delaye, J.C.Launay, and G.Roosen, Opt. Commun, Vol. **93**, p. 59, 1992.

13. A.S.Jordan and J.M.Parsey, Jr. MRS Bulletin , Oct. 1988, p.36-43.

14. G.M. Martin, Appl. Phys. Lett., Vol. **39**, p. 747-748, 1981.

15. P. Dobrilla and J.S. Blakemore, J. Appl. Phys., Vol. **58**, p. 208-218, 1985.

16. R. N.Thomas, S.McGuigan, G.W.Eldridge, and D.L.Barret, Proc. IEEE, **76**, p.778-791, 1988.

17. A.Partovi, E.M.Garmire, and L.J.Cheng, Appl. Phys. Lett., **51**, p.299-301, 1987

18. K. Jarasiunas and J. Vaitkus, Phys. Stat. Sol. (a), Vol. **44**, p. 793, 1977.

19. K.Jarasiunas and H.J.Gerritsen, Appl.Phys. Lett., **33**, p.190-193, 1978.

20. EC studies in SI LEC-grown GaAs by using nanosecond pulses of YAG-laser have shown that the decrease of transmittivity with excitation was correlating with the essential increase of the slope γ ; see : K. Jarasiunas, L. Jonikas, R. Reksnys, J. Storasta, J. Vaitkus, and R. Vasiliauskas. Annales Universitatis Mariae Curie-Sklodowska, Lublin, Polonia, Vol. **43/44**, sectio AAA, p. 83-91, 1988/89.

21. L.Disdier and G.Roosen, Opt. Commun., **88,** 559-568 (1992).

22. G.C.Valley, J.Dubard, and A.L.Smirl, IEEE J. Quantum. Electron. **QE-26**, 1058 (1990).

23. E.Garmire, D.F.Lovelace, and G.B.Thompson, Appl.Opt. **15**, 1394-97, 1976.

24. G.C. Valley, T.F. Boggess, J. Dubard and A.L. Smirl, J. Appl. Phys. , Vol. **66**, p. 2407-2413, 1989.

25. M.Pugnet, J.Collet, and B.Saint Cricq, Europhys. Lett. **7**, 567 (1988).

26. M.Kaminska, M.Skornowski, J.Lagowski, J.M.Parsey and H.C.Gatos, Appl. Phys.Lett., **43**, p.302-304, 1983.

27. G.A.Barraf, and M.A.Shluter, Phys. Rev. B, **45**, p.8300-09, 1992.

28. P.Omling, P.Silverberg, and L.Samuelson, Phys. Rev. B, **38**, p.3606-09, 1988.

29. B. Dischler and U. Kaufmann, Revue Phys. Appl., Vol. **23**, p. 779-791, 1988.

30. J.Dabrowski and M.Scheffler, Phys. Rev. B, **40**, pp.10391-401, 1989.

31. J.C.Fabre, J.M.C.Jonathan, G.Roosen,J.Opt. Soc. Am. B, **8**, p.1730-1736, 1988.

32. A.M.Glass, D.von der Linde, and T.J.Negran, Appl. Phys. Lett., **25**, p.233-35, 1974.

33. D.Ferré and J.-L.Farvacque, Revue Phys. Appl., **25**, p.323-332, 1990.

34. J.-L. Farvacque and B.Podor, Phys. Stat. Sol. (b), **167**, p. 687, 1991.

FIGURE CAPTIONS

Fig. 1 Experimental set-up : G.P. : Glan Polarizer, $\lambda/2$: half wave plate, D : Detector.

Fig. 2 Exposure characteristics of light diffraction on free carrier gratings (1a, 1b) and of sample transmittivity (2) . The p-polarized probe beam delay time is Δt= 26 ps (1a and 2) and Δt=170 ps (1b); for crystal orientation K_g along (110).

Fig. 3 Exposure characteristics of light diffraction on photorefractive gratings (1) and of sample transmittivity (2) . The s-polarized probe beam delay time is Δt=26 ps and the sample orientation corresponds toK_g along (110).

Fig. 4. Dynamics of light induced change in transmittivity of the sample for p-polarized (1) and for s-polarized (2) probe beam at excitation fluence of 8 mJ.cm^{-2}.

Fig. 5 Free carrier grating dynamics at low excitation levels: E= 0.88±0.12 mJ.cm^{-2} (1), 1.12 ±0.12 mJ.cm^{-2} (2), 1.62 ± 0.12 mJ.cm^{-2} (3).

Fig. 6 Free carrier grating dynamics at high excitation levels:
(a) E= 3.25 ±0.25 mJ.cm^{-2} (1), 5.5 ±0.5 mJ.cm^{-2} (2)
(b) 8.5 ± 0.5 mJ.cm^{-2}.

Fig. 7. Grating decay times due to carrier diffusion (1) and drift (2) calculated by using the parameters of experiment : carrier mobilities in undoped GaAs ($\mu_e \approx$5200 cm^2.V^{-1}.s^{-1}, $\mu_h \approx$400 cm^2.V^{-1}.s^{-1}) and grating period Λ =1.8 μm.

Fig. 8 Photorefractive grating dynamics at different excitation levels :
(a) 2.25 ± 0.25 mJ.cm^{-2} (1) and 2.75 ± 0.25 mJ.cm^{-2} (2) ;
(b) 6.75 ± 0.25 mJ.cm^{-2} (1) and 8.5± 0.5 mJ.cm^{-2} (2).

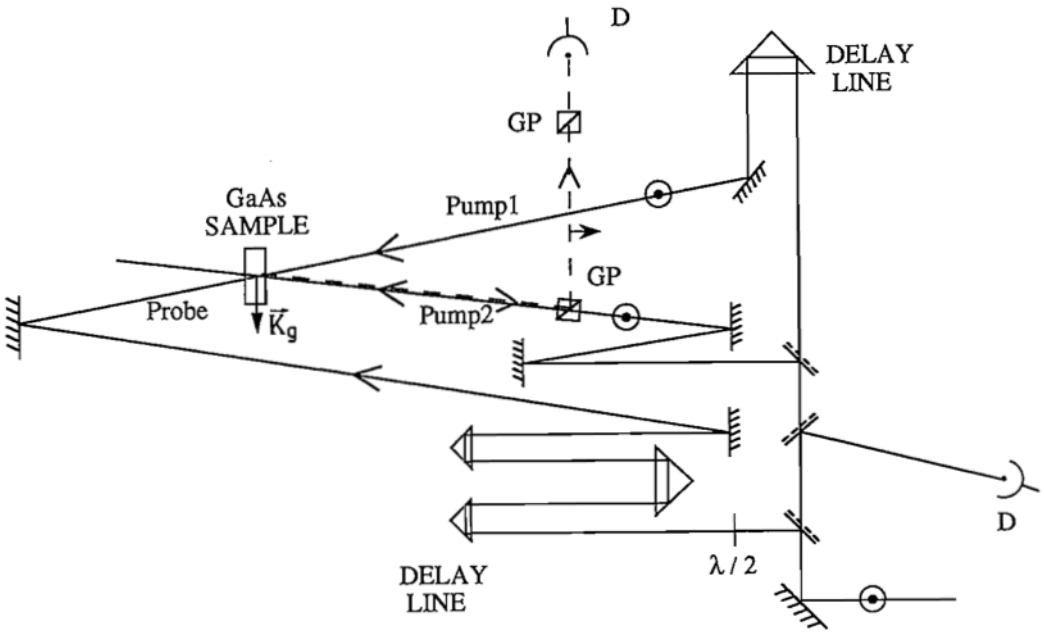

Figure 1

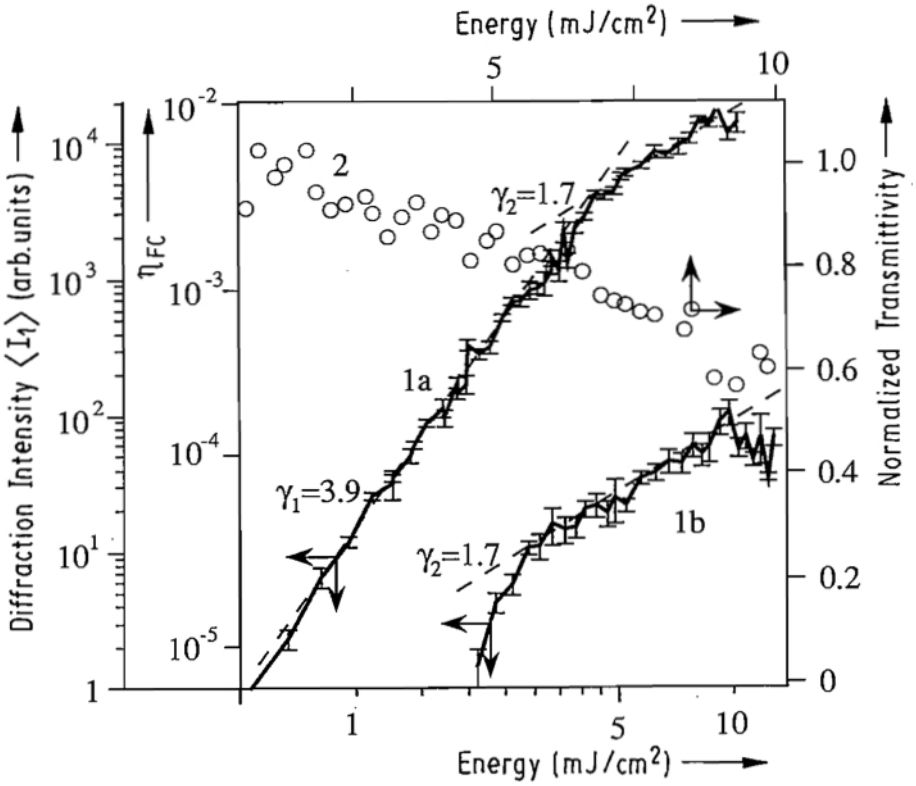

Figure 2

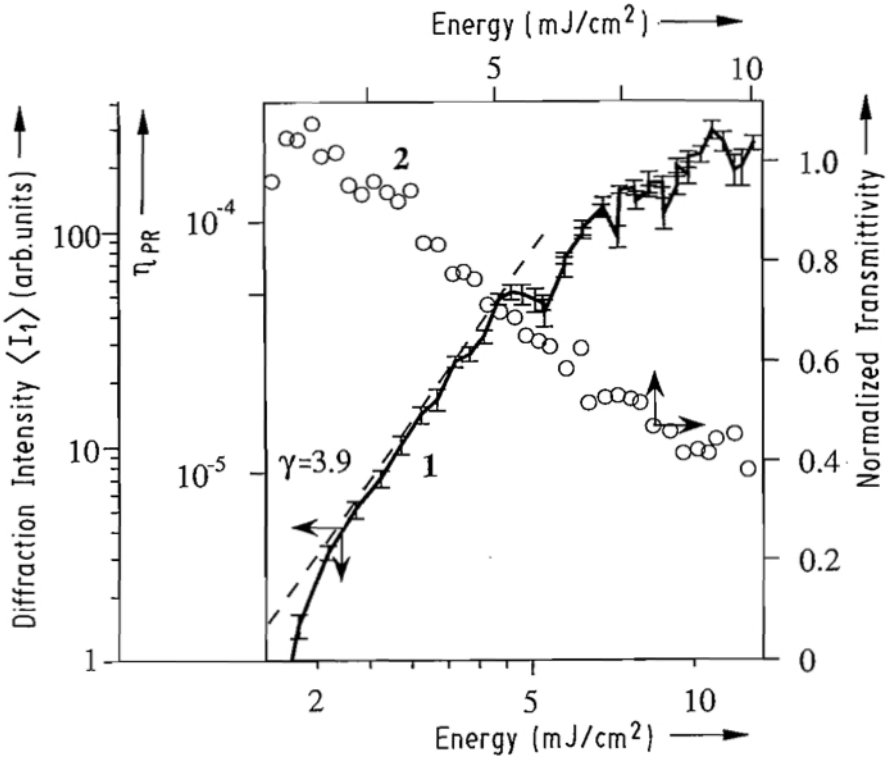

Figure 3

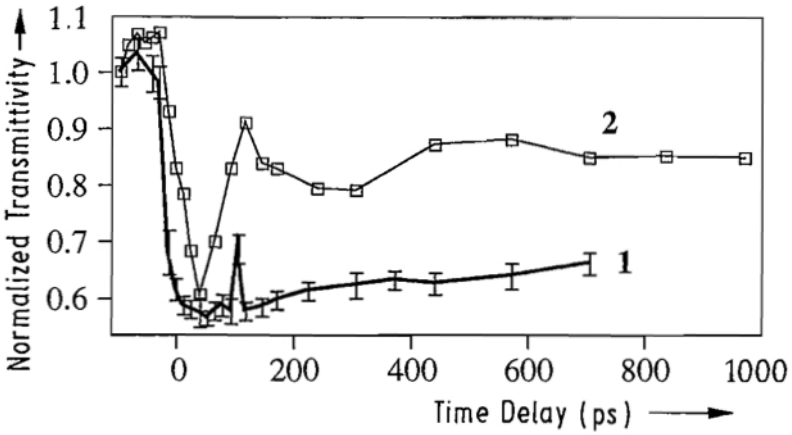

Figure 4

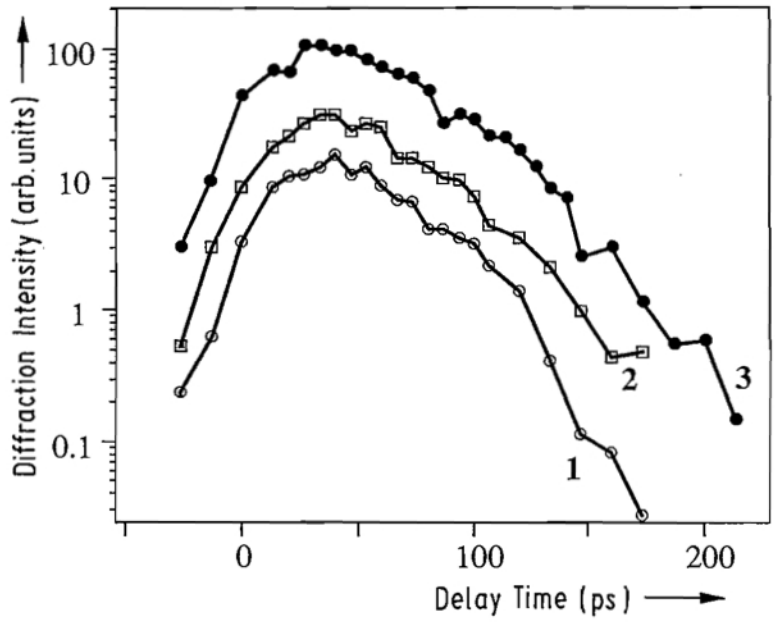

Figure 5

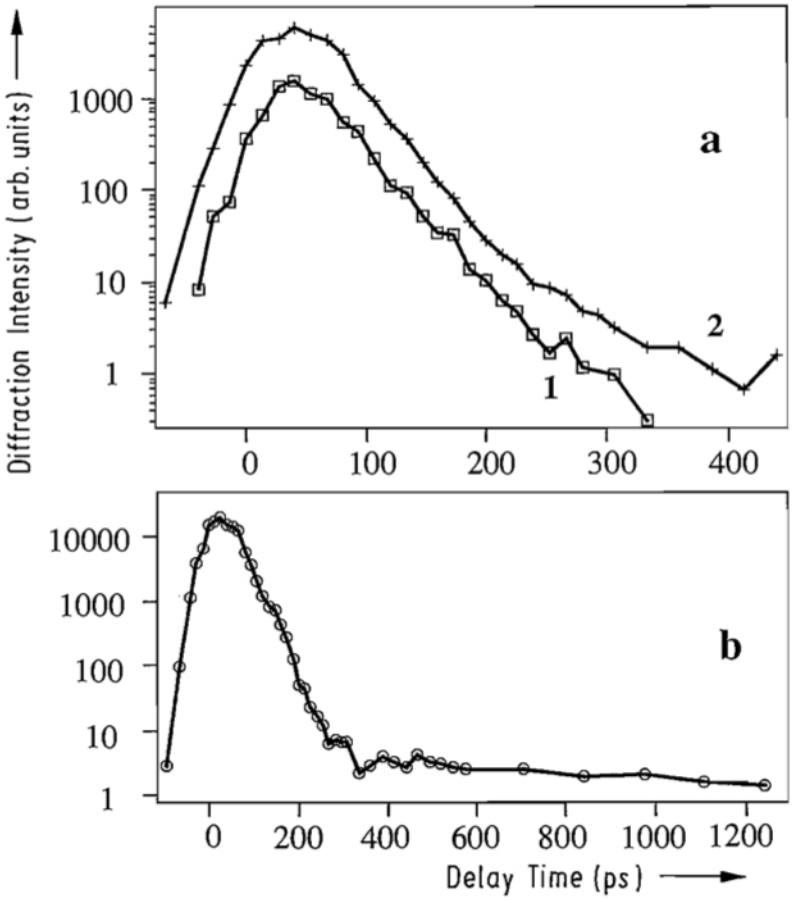

Figure 6

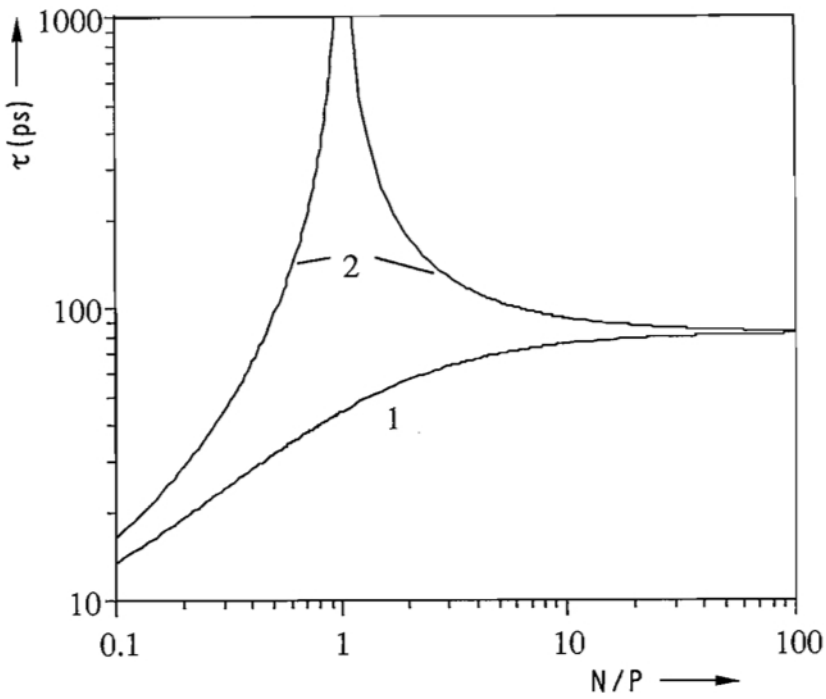

Figure 7

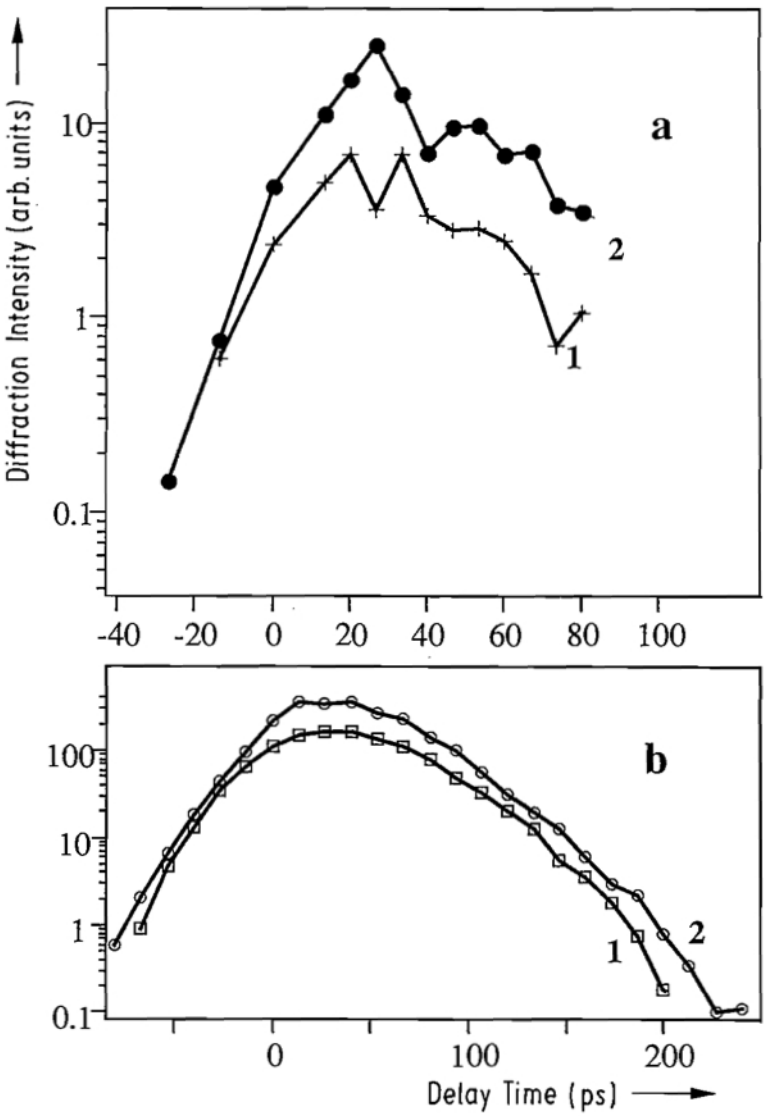
Diffraction Intensity (arb. units)
10
1
0.1
a
2
1
-40
-20
0
20
40
60
80
100
100
10
1
0.1
b
2
1
0
100
200
Delay Time (ps)

Figure 8